

Title: SARS-CoV-2 genome evolution exposes early human adaptations

Running title: SARS-CoV-2 routes of human adaptation

Erik S. Wright^{1,2,*}, Seema S. Lakdawala^{3,4}, & Vaughn S. Cooper^{2,3}

¹ Department of Biomedical Informatics, University of Pittsburgh

² Center for Evolutionary Biology and Medicine, Pittsburgh, PA, USA

³ Department of Microbiology and Molecular Genetics, University of Pittsburgh

⁴ Center for Vaccine Research, Pittsburgh, PA, USA

* Corresponding author email: eswright@pitt.edu

1 ABSTRACT

2 The set of mutations observed at the outset of the SARS-CoV-2 pandemic may illuminate how
3 the virus will adapt to humans as it continues to spread. Viruses are expected to quickly acquire
4 beneficial mutations upon jumping to a new host species. Advantageous nucleotide
5 substitutions can be identified by their parallel occurrence in multiple independent lineages and
6 are likely to result in changes to protein sequences. Here we show that SARS-CoV-2 is acquiring
7 mutations more slowly than expected for neutral evolution, suggesting purifying selection is the
8 dominant mode of evolution during the initial phase of the pandemic. However, several parallel
9 mutations arose in multiple independent lineages and may provide a fitness advantage over the
10 ancestral genome. We propose plausible reasons for several of the most frequent mutations.
11 The absence of mutations in other genome regions suggests essential components of SARS-
12 CoV-2 that could be the target of drug development. Overall this study provides genomic
13 insights into how SARS-CoV-2 has adapted and will continue to adapt to humans.

14

15 SUMMARY

16 In this study we sought signals of evolution to identify how the SARS-CoV-2 genome has
17 adapted at the outset of the COVID-19 pandemic. We find that the genome is largely
18 undergoing purifying selection that maintains its ancestral sequence. However, we identified
19 multiple positions on the genome that appear to confer an adaptive advantage based on their
20 repeated evolution in independent lineages. This information indicates how SARS-CoV-2 will
21 evolve as it diversifies in an increasing number of hosts.

22 INTRODUCTION

23 A better understanding of the origin and evolution of the SARS-CoV-2 pandemic may
24 help to mitigate disease outbreaks. Initial genome comparisons point toward a proximal origin
25 in horseshoe bats (1), with possible intermediate hosts including pangolins, cats, and ferrets (2-
26 4). Differences between host species are believed to present many barriers to host switching,
27 likely resulting in a virus that is initially maladapted to a new host (5, 6). Viruses are expected to
28 quickly adapt to a new species via mutations that increase transmissibility and decrease the
29 serial interval (7). Yet, relatively little is known about the mode and tempo of evolution at the
30 start of many epidemics, including the SARS-CoV-2 pandemic. Owing to the relatively high
31 mutation rates of RNA viruses, comparison of genome sequences may reveal a wealth of
32 information even at early stages of an outbreak (8).

33 Previous studies suggest that new environments provide the opportunity to develop a
34 large number of beneficial mutations, which may accrue quickly due to natural selection (9).
35 High rates of adaptation have been observed for viruses propagated in cell lines belonging to
36 new host species (10). The possibility of an adaptive advantage over the ancestor gives rise to
37 three outcomes: (i) increasing frequencies of beneficial mutations, (ii) parallel evolution, where
38 the same mutation rises to detectable frequencies in different lineages, and (iii) positive
39 selection, where the number of non-synonymous changes exceeds the number of synonymous
40 changes in protein coding regions of the genome. Mutations can rise in frequency for reasons
41 other than positive selection, such as arising by chance near the outset of a pandemic or after
42 undergoing a bottleneck when invading a new population of susceptible hosts. It is also
43 challenging to accurately determine mutant frequencies due to an uneven sampling of

44 genomes. Therefore, repeated parallel evolution is a clearer signal of adaptation than changes
45 in frequency. Evidence of parallel evolution also enables identification of beneficial mutations
46 before they have had time to substantially rise in frequency, which is particularly useful at the
47 beginning of a pandemic.

48 At the other end of the spectrum is the mode and tempo of evolution that is expected
49 when an organism is well-poised to enter a new environment or has spent a long time adapting
50 to a specific context. In such cases we anticipate evolution to occur slowly because further
51 mutation would not provide an advantage over recent ancestors. This would appear in the
52 genome as neutral or purifying selection, where the number of non-synonymous changes does
53 not exceed the number of synonymous changes at protein coding sites. Invasion into an
54 environment where an organism was already well-suited would cause a bottleneck event that
55 results in a homogenous population and a low rate of divergence due to purifying, or negative
56 selection. Therefore, the frequency and type of mutations at the outset of a pandemic can
57 provide insight into the ways in which a pathogen is initially well-adapted or maladapted,
58 potentially informing the development of therapies that target its weaknesses and avoid
59 resistance evolution.

60 RESULTS AND DISCUSSION

61 *SARS-CoV-2 is undergoing purifying selection*

62 Based on previous studies from similar coronaviruses, SARS-CoV-2 is anticipated to have
63 a relatively low per-base pair mutation rate for RNA viruses, resulting in approximately 1
64 mutation per genome replication (11-13). We estimated an average viral replication time of 6
65 hours based on SARS-CoV-2 titers and the known replication times of similar viruses (14).

66 Therefore, we would expect mutations to accumulate on the order of ~4 per day under neutral
67 evolution and potentially faster under positive selection. In contrast, we observe the number of
68 nucleotide substitutions increasing at a rate of approximately 0.062 per day (Fig. 1). This
69 equates to 8×10^{-4} per site per year, which is similar in magnitude to other RNA viruses and
70 indistinguishable from that of SARS-CoV (15). This result implies that purifying selection
71 dominated during the early stages of the SARS-CoV-2 pandemic. However, it does not rule out
72 the possibility that some sites are under positive selection even if most remain under negative
73 selection.

74 *Mutational and selection biases across the SARS-CoV-2 genome*

75 Beneficial mutations can be readily identified in laboratory evolution experiments
76 through parallel mutations that arise in multiple independent replicates (16, 17), also known as
77 homoplasies. We applied this intuition to search for beneficial mutations in the SARS-CoV-2
78 genome as it diversifies across many hosts. As shown in Figure 2, we observed 6,028 positions
79 with substitutions out 29,903 nucleotides in the genome (Fig. 2a). Of these, 2,070 positions had
80 more than one independent substitution, 1,858 of which were located in coding regions.
81 Substitutions displayed a strong bias toward guanine (G) and cytosine (C) being replaced with
82 uracil (U) in the genome (Fig. S1). U replacing C was 2.5-fold more common than the reverse,
83 and U replacing G was 6.4-fold more common than the reverse. C to U transitions accounted for
84 31% of substitutions, and may result from effects of the APOBEC3G gene causing deamination
85 of C to U (18). G to U substitutions represented 43% of transversions, although the cause of
86 their relatively high frequency was unknown.

87 Non-synonymous substitutions represented 66% of substitutions in coding regions.

88 Based on the frequency of codons and observed substitution rates, we estimated that non-

89 synonymous substitutions would represent 71% of substitutions without selection against

90 changes to the protein sequence. Therefore, the slight bias toward non-synonymous

91 substitutions is lower than expected and consistent with purifying selection being the dominant

92 mode of evolution. However, the skew toward non-synonymous substitutions varied across the

93 genome (Fig. 2a), reaching a peak within the gene coding for the nucleocapsid protein N that

94 protects the viral RNA. In contrast, genes with a bias toward synonymous substitutions, such as

95 the membrane protein M, indicate their protein sequence is relatively constrained.

96 We observed several conserved regions that displayed a relative lack of mutations (Fig.

97 2a), including the C-terminus of nsp3 (1,880 – 1,959), the N-terminus of nsp10 (2 – 59), a

98 central region within the RNA polymerase nsp12 (504 – 570), and a region within the spike

99 protein S (976 – 1,041). The conserved region within nsp12 overlaps with the entry tunnel for

100 the RNA template (19) and the predicted binding sites of many antivirals (20, 21). The

101 conserved region within S encompasses the central helix (22), which is believed to initiate the

102 fusion of viral and host membranes (23). These conserved regions may offer reasonable drug

103 targets because they are more likely to avoid the evolution of drug resistance.

104 *Evidence of adaptation at multiple genome positions*

105 The observation of parallel evolution in independent lineages enables us to pinpoint

106 specific genome positions that likely increase the fitness of SARS-CoV-2 in the human host. The

107 extreme 5' and 3' ends of the genome contained the highest concentration of parallel

108 substitutions (Fig. 2a). Despite their high frequencies, these substitutions were observed

109 exclusively in genomes originating from the same laboratory, which suggests they are
110 sequencing errors rather than authentic mutations. Therefore, we chose to focus on
111 substitutions found in genomes from at least four of the 529 contributing laboratories to
112 mitigate the presence of lab-specific sequencing errors.

113 We observed two substitutions with more than 30 cases of parallelism across SARS-CoV-
114 2 genomes (Fig. 2b). The most frequent substitution occurred 50 different times at position
115 11,083, which results in a non-synonymous change (L37F) in nsp6, a transmembrane protein
116 localized to the endoplasmic reticulum and implicated in formation of autophagosomes (24-27).
117 The substitution at 11,083 occurred nearby another frequent substitution at position 11,074
118 that is synonymous. Both substitutions were conversions to uracil at sites adjacent to eight
119 consecutive uracils in the genome (Fig. 3), suggesting they may occur more frequently due to an
120 increased mutation rate at homopolymeric sites (28). A similar conversion to uracil at position
121 21,575 is located in the middle of 7 other uracils and results in a non-synonymous change (L5F)
122 to the protein sequence of S (Fig. 3). Three other substitutions were adjacent to at least 3
123 uracils in the genome: positions 9,474, 26,681, and 28,253. The high frequency of substitutions
124 next to poly(U) tracts is likely due to increased mutation rates at these positions, although we
125 cannot rule out that they may also have adaptive significance.

126 The next most frequent substitution occurred 16 times at position 16,887 and results in
127 a synonymous change to nsp3. There is presently no evidence that this mutation is involved in
128 RNA base pairing, and it is located in a region of the genome with relatively little conserved RNA
129 secondary structure (29). The most frequent non-C-to-U substitution was A10323G, which
130 results in a non-synonymous change (K90R) to the protease nsp5. This amino acid replacement

131 is distally located from the active site and the nsp5 dimer interface (30), suggesting it may not
132 be of adaptive significance. We observed a similar substitution, A21137G, which results in a
133 non-synonymous change (K160R) to nsp16. However, this residue is distant from the active site
134 and from the nsp16/nsp10 interface (31), suggesting its replacement could be of little
135 consequence.

136 Two different nonsynonymous mutations in the N gene, encoding the nucleocapsid
137 protein, repeatedly evolved in a disordered linker domain between structural capsid elements
138 (32). These mutations, R185C and T205I, alter a region acting as an RNA chaperone that
139 facilitates template switching and RNA synthesis during replication (33, 34). Similarly intriguing,
140 we observed divergent nucleotide substitutions, G28077C/U, that both result in the same non-
141 synonymous change (V62L) to ORF8. This region of ORF8 is missing in some SARS-related
142 viruses (Fig. 3), and underwent repeated deletions during the SARS-CoV epidemic (35). ORF8 is
143 known to rapidly evolve and the necessity of its role in the human host remains contentious
144 (36).

145 We sought to determine whether any of these eighteen highly parallel mutations (Fig.
146 2b) could be attributable to common sequencing errors. We reasoned that sequencing errors
147 would be randomly distributed across the phylogenetic tree, whereas adaptive mutations are
148 likely to expand in size along a specific lineage. Therefore, we calculated the probability of
149 finding a mutant clade of size R or larger by chance given each substitution's observed
150 frequency. For example, the substitution G11074U had a largest clade size of R=4, for which we
151 observed 24 mutants among 12,435 genomes. In this case, the probability of observing four or
152 more adjacent mutants on the phylogenetic tree is much less than 10^{-6} . Extremely small p-

153 values were found for all parallel substitutions reported here, except the mutation at 9,474
154 which was only supported by singletons (R=1).

155 In this study, we determined that SARS-CoV-2 is evolving predominantly under purifying
156 selection that purges most mutations since they are deleterious. This suggests that SARS-CoV-2
157 was well-poised to invade the human population, although it continues to adapt to humans
158 through specific mutations that may accumulate in individual genomes as SARS-CoV-2
159 continues to evolve. The few highly parallel substitutions that we observed offer intriguing
160 avenues for further investigation, as most are cryptic and located in poorly characterized
161 regions of the SARS-CoV-2 genome. Notably, some genes acquired relatively few mutations,
162 which implies strict sequence constraints that may focus drug development strategies against
163 these gene products. The paucity of mutations overall suggests that coronaviruses are well-
164 suited to jumping between hosts and caution should be taken to avoid direct or indirect contact
165 with their animal reservoirs. This is further corroborated by the relatively small number of
166 genome positions that have undergone multiple parallel substitutions despite a plentiful supply
167 of mutations.

168 METHODS

169 *Genome collection and comparison*

170 Complete (> 29,000 nucleotide) SARS-CoV-2 genomes were downloaded from GISAID
171 (37) on May 2nd, 2020. Genomes with more than 500 degeneracies (e.g., N's) were removed,
172 resulting in a collection of 12,435 genomes, of which 12,285 had a known date of collection
173 that we used as a proxy for the duration of growth relative to the first genome (2019-12-24).
174 Genomes were aligned to the SARS-CoV-2 reference genome (NC_045512.2) using the

175 DECIPHER (v2.16.1) (38, 39) package for the R (v3.6.1) programming language (40). Genomic
176 distance was defined as the number of positions differing from the reference genome without
177 considering insertions or deletions, which were very infrequent.

178 To create Figure 4, viruses closely related to SARS-CoV-2 were selected from a recent
179 study (1) and supplemented with one sequence derived from a pangolin host in another study
180 (2). Genomes were aligned and a maximum likelihood tree was created using DECIPHER with
181 the best fitting evolutionary model.

182 *Identification of parallel substitutions across independent lineages*

183 Starting from the set of all SARS-CoV-2 genomes, we constructed a multiple sequence
184 alignment, matrix of pairwise nucleotide identity, and rooted neighbor joining tree using
185 DECIPHER. Sequences were compared at each site in the reference sequence to identify
186 independent substitutions on the phylogenetic tree. That is, we mapped mutations onto tips of
187 the phylogenetic tree and propagated them back till they coalesced at a common ancestor
188 (edge). This enabled us to count the number of independent substitutions that were inherited
189 by one or more strains. To increase robustness to the tree topology, we ignored single
190 reversions to the ancestral character that occurred within a clade sharing a derived character.

191 This process resulted in an integer representing the number of parallel substitutions
192 occurring at each position in the reference sequence. We determined that eight or more
193 independent substitutions was statistically significant for C to U transitions ($p < 0.001$, Poisson
194 distribution and Bonferroni correction) given the observed mutations rates and assuming
195 mutations are randomly distributed along the genome. All other substitutions (e.g., G to U)
196 required fewer cases of parallelism to achieve the same degree of statistical significance.

197 Conserved regions were defined as stretches (≥ 100 nucleotides) of the genome where
198 the average number of independent substitutions fell below 0.2 (Fig. 2a). To improve the
199 identification of conserved regions, we applied a center-point moving average function that
200 smoothed the mutation signal across the genome. A similar process was used to determine the
201 bias in synonymous versus non-synonymous substitutions within protein coding regions (Fig.
202 2a). A fully reproducible and open source analysis pipeline is provided on GitHub
203 (<https://github.com/digitalwright/ncov>).

204 ACKNOWLEDGEMENTS

205 We are grateful for the contributions of laboratories involved in collecting samples and
206 creating the dataset made available by GISAID.

207 FUNDING

208 This study was funded by NIAID grants 1DP2AI145058-01 and 1R21AI144769-01A1 to
209 ESW and U01AI124302-01 to VSC. The funders had no role in study design, data collection and
210 analysis, decision to publish, or preparation of the manuscript.

REFERENCES

1. Coronaviridae Study Group of the International Committee on Taxonomy of Viruses, The species Severe acute respiratory syndrome-related coronavirus: classifying 2019-nCoV and naming it SARS-CoV-2. *Nat Microbiol* **5**, 536-544 (2020).
2. T. T. Lam *et al.*, Identifying SARS-CoV-2 related coronaviruses in Malayan pangolins. *Nature* **10.1038/s41586-020-2169-0** (2020).
3. K. G. Andersen, A. Rambaut, W. I. Lipkin, E. C. Holmes, R. F. Garry, The proximal origin of SARS-CoV-2. *Nature Medicine* **10.1038/s41591-020-0820-9** (2020).
4. J. Shi *et al.*, Susceptibility of ferrets, cats, dogs, and other domesticated animals to SARS-coronavirus 2. *Science* **10.1126/science.abb7015** (2020).
5. N. Mollentze, R. Biek, D. G. Streicker, The role of viral evolution in rabies host shifts and emergence. *Curr Opin Virol* **8**, 68-72 (2014).
6. P. Simmonds, P. Aiewsakun, A. Katzourakis, Prisoners of war - host adaptation and its constraints on virus evolution. *Nat Rev Microbiol* **17**, 321-328 (2019).
7. J. J. Bull, D. Ebert, Invasion thresholds and the evolution of nonequilibrium virulence. *Evol Appl* **1**, 172-182 (2008).
8. G. Dudas, T. Bedford, The ability of single genes vs full genomes to resolve time and space in outbreak analysis. *BMC Evol Biol* **19**, 232 (2019).
9. R. Lanfear, H. Kokko, A. Eyre-Walker, Population size and the rate of evolution. *Trends Ecol Evol* **29**, 33-41 (2014).
10. I. S. Novella *et al.*, Extreme fitness differences in mammalian and insect hosts after continuous replication of vesicular stomatitis virus in sandfly cells. *J Virol* **69**, 6805-6809 (1995).
11. A. E. Gorbalenya, L. Enjuanes, J. Ziebuhr, E. J. Snijder, Nidovirales: evolving the largest RNA virus genome. *Virus Res* **117**, 17-37 (2006).
12. R. Sanjuan, M. R. Nebot, N. Chirico, L. M. Mansky, R. Belshaw, Viral mutation rates. *J Virol* **84**, 9733-9748 (2010).
13. H. D. Song *et al.*, Cross-host evolution of severe acute respiratory syndrome coronavirus in palm civet and human. *Proc Natl Acad Sci U S A* **102**, 2430-2435 (2005).
14. Y. Pan, D. Zhang, P. Yang, L. L. M. Poon, Q. Wang, Viral load of SARS-CoV-2 in clinical samples. *The Lancet Infectious Diseases* **20**, 411-412 (2020).
15. Z. Zhao *et al.*, Moderate mutation rate in the SARS coronavirus genome and its implications. *BMC Evol Biol* **4**, 21 (2004).
16. D. I. Bolnick, R. D. H. Barrett, K. B. Oke, D. J. Rennison, Y. E. Stuart, (Non)Parallel Evolution. *Annual Reviews of Ecology, Evolution, and Systematics* **49**, 303-330 (2018).
17. C. B. Turner, C. W. Marshall, V. S. Cooper, Parallel genetic adaptation across environments differing in mode of growth or resource availability. *Evol Lett* **2**, 355-367 (2018).
18. R. Sanjuan, P. Domingo-Calap, Mechanisms of viral mutation. *Cell Mol Life Sci* **73**, 4433-4448 (2016).
19. Y. Gao *et al.*, Structure of the RNA-dependent RNA polymerase from COVID-19 virus. *Science* **10.1126/science.abb7498**, eabb7498 (2020).

20. A. A. Elfiky, Ribavirin, Remdesivir, Sofosbuvir, Galidesivir, and Tenofovir against SARS-CoV-2 RNA dependent RNA polymerase (RdRp): A molecular docking study. *Life Sci* 10.1016/j.lfs.2020.117592, 117592 (2020).
21. W. Yin *et al.*, Structural basis for inhibition of the RNA-dependent RNA polymerase from SARS-CoV-2 by remdesivir. *Science* 10.1126/science.abc1560 (2020).
22. D. Wrapp *et al.*, Cryo-EM structure of the 2019-nCoV spike in the prefusion conformation. *Science* **367**, 1260-1263 (2020).
23. R. N. Kirchdoerfer *et al.*, Stabilized coronavirus spikes are resistant to conformational changes induced by receptor recognition or proteolysis. *Sci Rep* **8**, 15701 (2018).
24. S. Baliji, S. A. Cammer, B. Sobral, S. C. Baker, Detection of nonstructural protein 6 in murine coronavirus-infected cells and analysis of the transmembrane topology by using bioinformatics and molecular approaches. *J Virol* **83**, 6957-6962 (2009).
25. E. M. Cottam *et al.*, Coronavirus nsp6 proteins generate autophagosomes from the endoplasmic reticulum via an omegasome intermediate. *Autophagy* **7**, 1335-1347 (2011).
26. J. A. EA, I. M. Jones, Membrane binding proteins of coronaviruses. *Future Virol* **14**, 275-286 (2019).
27. M. M. Angelini, M. Akhlaghpour, B. W. Neuman, M. J. Buchmeier, Severe acute respiratory syndrome coronavirus nonstructural proteins 3, 4, and 6 induce double-membrane vesicles. *mbio* **4** (2013).
28. M. M. Dillon, W. Sung, R. Sebra, M. Lynch, V. S. Cooper, Genome-Wide Biases in the Rate and Molecular Spectrum of Spontaneous Mutations in *Vibrio cholerae* and *Vibrio fischeri*. *Mol Biol Evol* **34**, 93-109 (2017).
29. R. Rangan, I. N. Zheludev, R. Das, RNA genome conservation and secondary structure in SARS-CoV-2 and SARS-related viruses. *bioRxiv* 10.1101/2020.03.27.012906 (2020).
30. Z. Jin *et al.*, Structure of M(pro) from COVID-19 virus and discovery of its inhibitors. *Nature* 10.1038/s41586-020-2223-y (2020).
31. E. Decroly *et al.*, Crystal structure and functional analysis of the SARS-coronavirus RNA cap 2'-O-methyltransferase nsp10/nsp16 complex. *PLoS Pathog* **7**, e1002059 (2011).
32. C. K. Chang, C. M. Chen, M. H. Chiang, Y. L. Hsu, T. H. Huang, Transient oligomerization of the SARS-CoV N protein--implication for virus ribonucleoprotein packaging. *PLoS ONE* **8**, e65045 (2013).
33. R. McBride, M. van Zyl, B. C. Fielding, The coronavirus nucleocapsid is a multifunctional protein. *Viruses* **6**, 2991-3018 (2014).
34. C. K. Chang *et al.*, Multiple nucleic acid binding sites and intrinsic disorder of severe acute respiratory syndrome coronavirus nucleocapsid protein: implications for ribonucleocapsid protein packaging. *J Virol* **83**, 2255-2264 (2009).
35. S. M. E. C. Chinese, Molecular evolution of the SARS coronavirus during the course of the SARS epidemic in China. *Science* **303**, 1666-1669 (2004).
36. D. Forni, R. Cagliani, M. Clerici, M. Sironi, Molecular Evolution of Human Coronavirus Genomes. *Trends Microbiol* **25**, 35-48 (2017).
37. S. Elbe, G. Buckland-Merrett, Data, disease and diplomacy: GISAID's innovative contribution to global health. *Glob Chall* **1**, 33-46 (2017).

38. E. S. Wright, Using DECIPHER v2.0 to Analyze Big Biological Sequence Data in R. *The R Journal* **8**, 352-359 (2016).
39. E. S. Wright, DECIPHER: harnessing local sequence context to improve protein multiple sequence alignment. *BMC Bioinformatics* **16**, 322 (2015).
40. R Core Team (2019) R: A Language and Environment for Statistical Computing. (R Foundation for Statistical Computing, Vienna, Austria).

FIGURES AND FIGURE LEGENDS

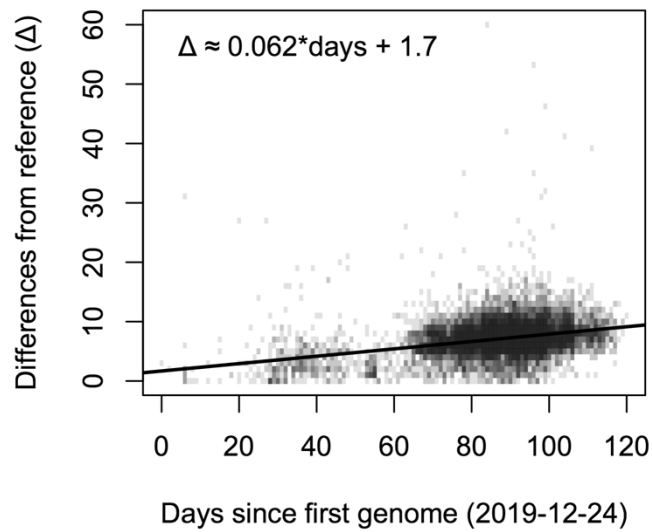


Figure 1. Rate of acquiring substitutions by SARS-CoV-2. The number of genomes with a given number of nucleotide substitutions relative to the reference genome (NC_045512.2) are shown since the first collected genome. The number of substitutions has increased at an average rate of approximately 0.062 substitutions per day (line of best fit), which is substantially lower than expected from a neutral model of evolution (~ 1 per day) and indicative of purifying selection.

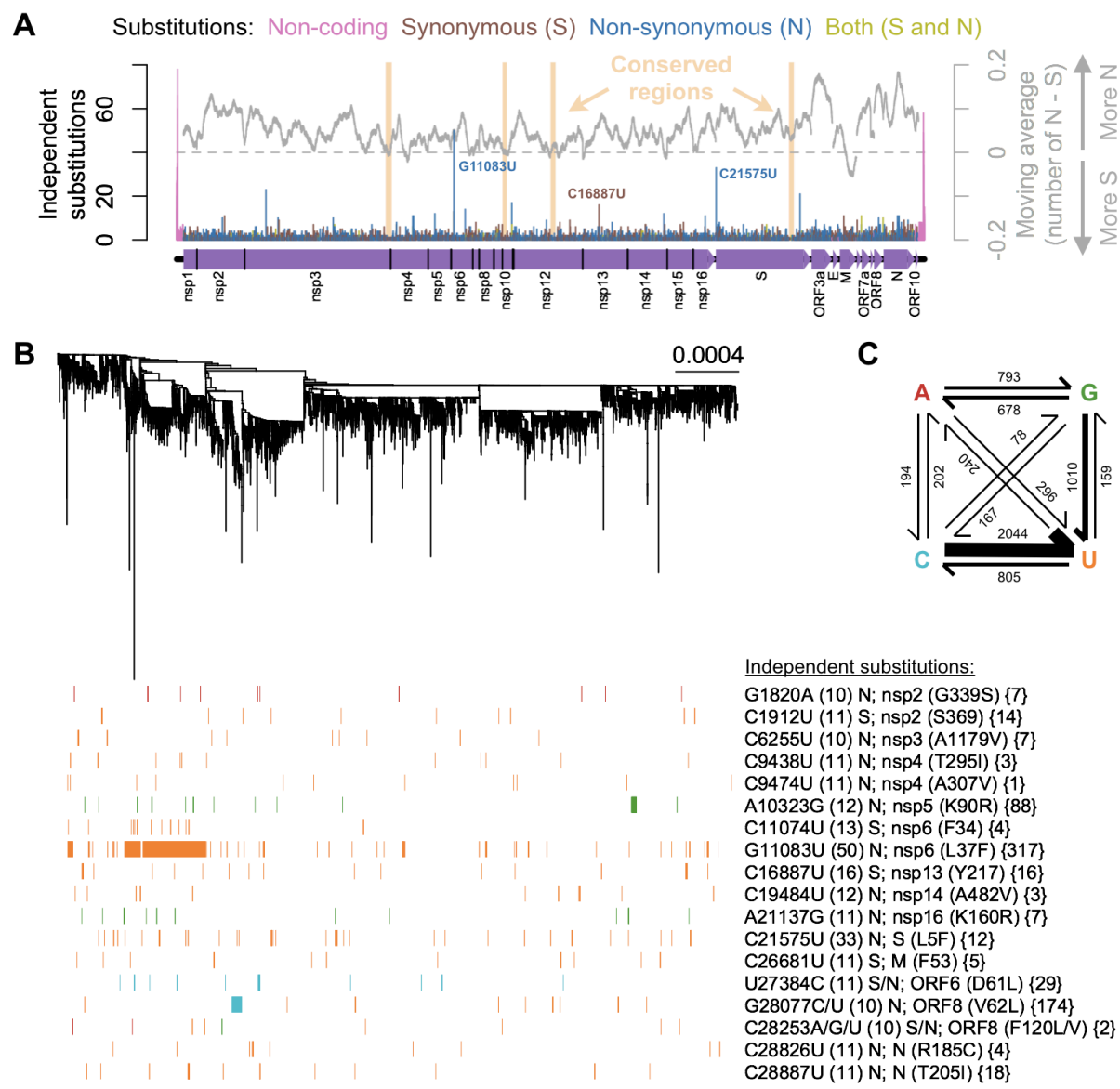


Figure 2. Mutational biases in the SARS-CoV-2 genome. (A) Independent substitutions were unevenly distributed along the genome, with a high concentration of parallel mutations near the genome termini and a paucity of substitutions in some coding regions. Long (≥ 100 nucleotide) conserved regions with few substitutions indicate where the genome is more constrained and could be the focus of drug targets that avoid resistance development. Some proteins (e.g., M) displayed a bias toward synonymous substitutions, suggesting the dominance of purifying selection purging changes to the protein sequence. (B) The pattern of parallel substitutions with 10 or more independent occurrences (number in parentheses) across a rooted phylogenetic tree built from SARS-CoV-2 genomes. Of these 18 substitutions, 14 change the protein sequence (N) and four are synonymous (S). The size of the largest clade associated with each mutation is shown in braces. (C) The matrix of substitutions shows a bias toward cytosine or guanine to uracil mutations.

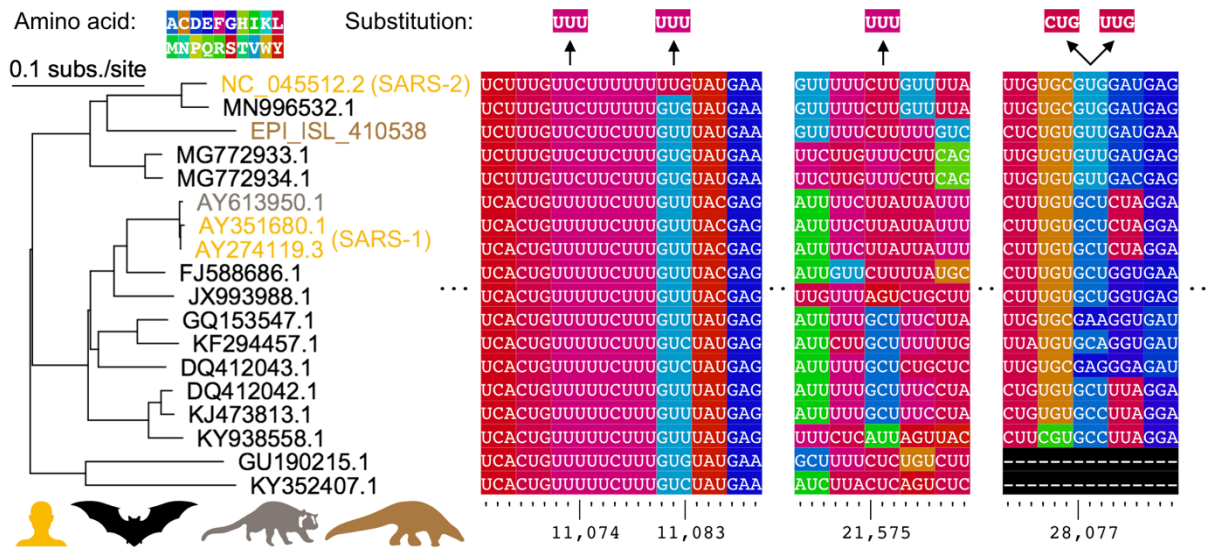


Figure 3. Comparative genomics of parallel substitutions in protein coding regions. A midpoint rooted maximum likelihood phylogenetic tree constructed from SARS-related coronavirus genome sequences with accession numbers colored by host species (human, bat, masked palm civet, or pangolin). Codons are colored by their corresponding amino acid with frequent nucleotide substitutions shown relative to the reference SARS-CoV-2 sequence (top). Poly(U) sequences are found surrounding the substitutions at positions 11,074, 11,083, and 21,575. The two substitutions observed at position 28,077 result in conversions to the same amino acid in ORF8.